

Phase-resolved spectral-domain magnetomotive optical coherence tomography

Vasilica Crecea^{1,2}, Amy L. Oldenburg^{1,3}, Tyler S. Ralston^{1,3}, Stephen A. Boppart^{1,2,3,4,*}

¹Biophotonics Imaging Laboratory, Beckman Institute for Advanced Science and Technology

²Department of Physics

³Department of Electrical and Computer Engineering

⁴Departments of Bioengineering, Medicine
University of Illinois at Urbana-Champaign

ABSTRACT

We advance the magnetomotive-optical coherence tomography (MM-OCT) technique for detecting displacements of magnetic nanoparticles embedded in tissue-like phantoms by using amplitude and phase-resolved methods with spectral-domain optical coherence tomography (SD-OCT). The magnetomotion is triggered by the external, noninvasive application of a magnetic field. We show that both amplitude and phase data are indicative of the presence and motion of light scatterers, and could potentially be used for studying the dynamics of magnetomotion. The magnetic field modulation is synchronized with data acquisition in a controlled, integrated system that includes a console for monitoring and initiating data acquisition, scanning devices, an electromagnet power supply, and the detection system. Using Fourier analysis, we show that the amplitude and phase modulations in the samples that contain magnetic contrast agents match the frequency of the applied magnetic field, while control samples do not respond to magnetic field activity. We vary the strength of the magnetic field and show that the amplitude and phase steps between regions of zero-magnetic field and regions with non-zero magnetic field change accordingly. The phase is shown to be more sensitive.

Keywords: Optical coherence tomography, phase detection, sensitivity, contrast agents, magnetic nanoparticles

INTRODUCTION

Optical coherence tomography (OCT)^{1,2} greatly benefits from the presence of contrast agents within the probed medium.³⁻⁵ Furthermore, specificity of contrast agents enhances the capabilities of OCT by selectively labeling biological units such as certain groups of molecules or cells. With proper targeting, this could eventually become a tool for differentiating between normal and pathologic tissue. Moreover, OCT imaging of tissue probed with such contrast agents could provide real-time feedback for diagnosis and surgical guidance.

The integrity of biological systems needs to be protected when subjected to various tests, including those using contrast agents. To this end, one needs to exercise vigilance when choosing a contrast agent, as effective non-invasive probing is desirable. Magnetic nanoparticles have been shown to be promising candidates for contrast agents in biomedical imaging,^{6,7} and in particular for OCT,⁸ due to their versatility and compliance with biosafety requirements. Toxicology studies conducted on magnetite nanoparticles lead to FDA approval in 1996, a matter of importance. Superparamagnetic iron oxide (SPIO) nanoparticles have already been used extensively as contrast agents for magnetic resonance imaging (MRI) in biology and medicine.⁹ Nanoparticles with small core sizes (<100nm) exhibit transport through the circulatory system and passage through the endothelium, without alteration of the nanoparticles' magnetic properties. The nanoparticles are very responsive to external, non-invasive manipulation or detection due to their strong magnetic susceptibility. They are also suitable for both *in vivo* and *in vitro* studies.^{6,8} These are the main reasons why we chose to work with magnetite nanoparticles of ~25nm size (Fig. 1). Reliable and

* For correspondence with Prof. Stephen A. Boppart email: boppart@uiuc.edu phone: (217) 244-7479

sensitive methods for characterizing their behavior and that of the surrounding biological medium are presently needed.

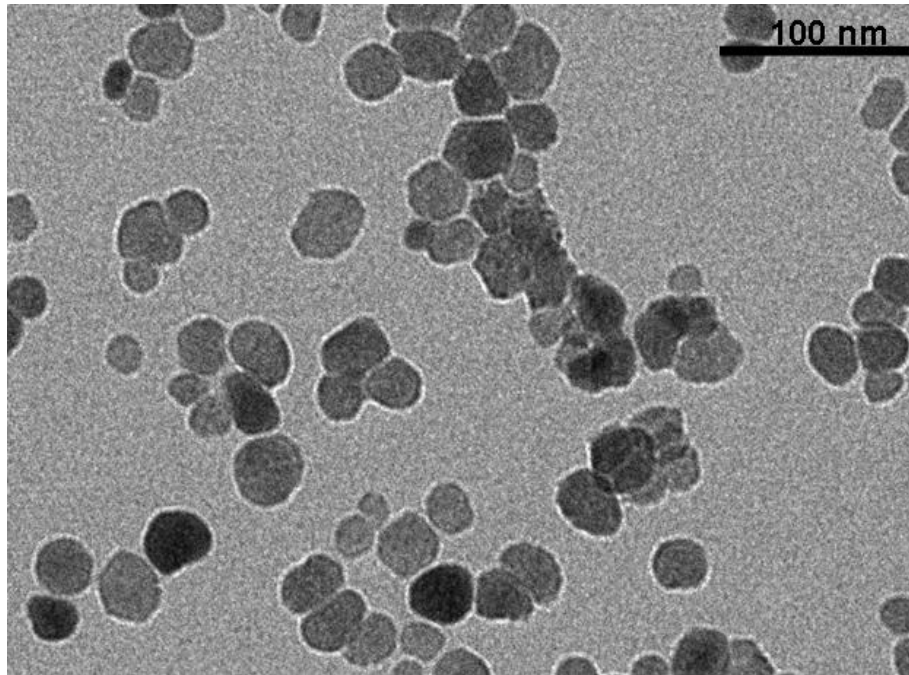


Figure 1: Transmission electron micrograph of magnetite nanoparticles used in MM-OCT studies.

Phase measurements in common-path low-coherence light interferometry have been shown to render high sensitivity to sub-wavelength displacements or obstacles in the path of light.¹⁰⁻¹² Path length sensitivities as low as 25 pm for spectral-domain optical coherence phase microscopy (SD-OCPM)¹⁰ and 18 pm (equivalent phase stability = 0.4 mrad) for spectral-domain phase microscopy (SDPM)¹¹ have been reported. Phase-resolved methods¹⁰⁻¹⁵ are often used in a dynamical regime, such as in measuring Intralipid¹⁶⁻¹⁸ or blood flow¹⁹⁻²³ velocities, nerve displacements,²⁴ or monitoring cell¹⁰ and even cardiomyocyte¹² activity. These remarkable results suggest that phase measurements in a spectral-domain OCT system are an appropriate approach for studying the dynamics of magnetomotion in MMOCT.

When embedded in tissue that is subsequently probed with an external magnetic field, magnetic nanoparticles move along the axis on which the field has a dominant gradient.⁴ In the present sample-magnetic field configuration, the magnetic field at the site being probed has a dominant vertical component along which it varies, engaging the magnetic nanoparticles in motion on a preferred direction normal to the top surface of the sample, which is also parallel to the probing beam. Magnetomotive optical coherence tomography (MM-OCT) in a time-domain optical coherence tomography (TD-MMOCT) system has been used to image such samples and it has been subsequently shown that the behavior of the nanoparticles is predictable.⁸ In this scheme, axial scans in a two-dimensional transversal sample plane were acquired with the magnetic field off and on, while allowing the particles sufficient time to complete motion and reach equilibrium between axial scans. Thus, the images taken with the time-domain MM-OCT system represent a static description of the sample in the absence and in the presence of the magnetic field. Experimental verification relied on analysis of amplitude changes that revealed magnetic field-induced motion in the samples of interest. The magnetomotive signal for control samples with no magnetic nanoparticles was effectively zero.

Studying the dynamics of the magnetic nanoparticles is also valuable as it could shed light onto the micro-mechanical properties of the tissue that hosts them. The tissue exerts an elastic force that opposes the magnetic force on the nanoparticles and thus causes them to eventually come to rest. At equilibrium the elastic force and the magnetic force cancel out. Therefore, by knowing the magnetic force and deducing the displacements in the sample from OCT

measurements, we could infer the regional elastic modulus of the sample on the micron scale, and throughout its volume.⁸ However, before the nanoparticles reach equilibrium, they are typically engaged in a damped oscillation. The equilibrating time, which describes how fast the damping of the oscillation takes place, is directly proportional to the ratio between the viscosity of the medium and the Young's modulus. In order to study the dynamics of the magnetomotion we need to take advantage of the capabilities of a spectral-domain OCT system.

We have improved the imaging performance on samples infiltrated with magnetic nanoparticles by using phase-resolved spectral-domain detection techniques in order to achieve faster acquisition times and better sensitivity. Time-domain OCT systems are known to have poor phase stability due to the mechanical nature of the reference arm, a problem that is reduced in spectral-domain OCT systems because the reference-arm mirror is fixed.²⁵⁻²⁸ We want to take advantage of the high responsiveness of phase to obstacles in the light path, namely scatterers, and to their motion. In order to achieve dynamic mechanical actuation of the tissue, we take advantage of the magnetically-responsive scattering contrast agents that are bound to the scaffold and, therefore, engage the agent and local scaffold in motion once the state of the external magnetic field changes. Phase shifts could be indicative of small motion, on the order of tens of picometers.¹⁰⁻¹² Ultimately, phase analysis could be used to characterize the dynamics of magnetomotion in samples with different mechanical properties or with different strengths of the magnetic field.

METHODOLOGY AND RESULTS

In this study we used silicone-based samples whose optical and mechanical properties matched closely those of biological tissue, for example human skin.² Titanium dioxide (TiO_2) microparticles with a diameter of about one micron served as scatterers. Magnetite (Fe_3O_4) nanoparticles with a mean diameter between 20-30 nm were homogeneously dispersed in the sample medium for a magnetic sample (Fig. 2). A separate base stock was prepared for the control sample and no magnetic nanoparticles were added to it.

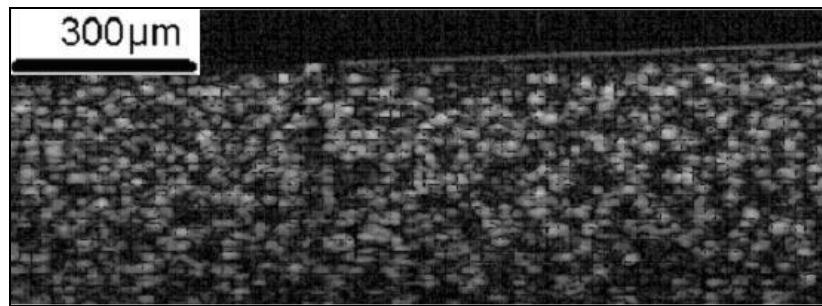


Figure 2: Amplitude OCT image of a tissue-like phantom showing presence of light scatterers throughout the volume.

The samples were probed with 13mW of optical power from a broadband titanium: sapphire laser (KMLabs, Inc.) centered at 800 nm and with a bandwidth of about 115 nm, providing an axial resolution of 3 μm . The magnetic field was applied by means of a computer-controlled electromagnet (Fig. 3) that was synchronized with the data acquisition and a lateral scanning mirror (the x galvanometer). The sample light was collimated through a 40 mm focal length achromatic lens, providing 16 μm lateral resolution. The magnetic nanoparticle concentration of the sample used in this study of the magnetomotion was 2.5 mg/g, as the response of this sample to changes in magnetic field were evident in amplitude data and phase data.

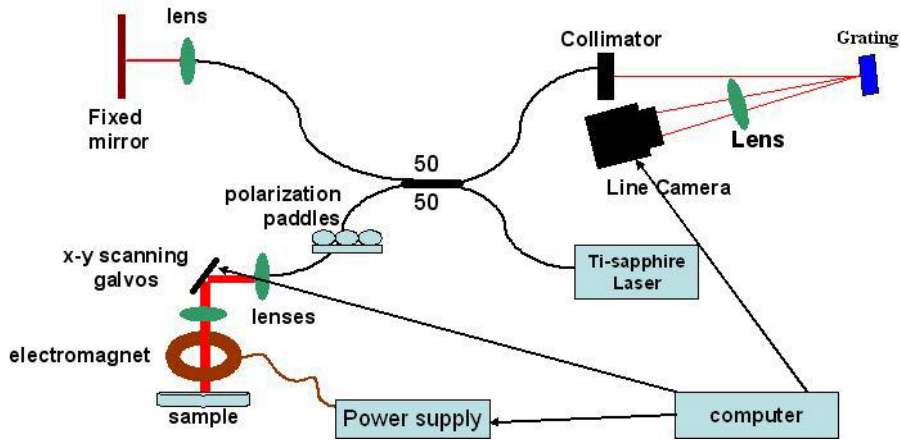


Figure 3: Diagram of experimental set up used for phase-resolved spectral-domain MM-OCT.

In a first set of experiments, spectral domain data was acquired in M-mode in order to reveal the time evolution of the amplitude and phase over a fixed vertical line in the sample, while the magnetic field was periodically turned on and off. Depth axial scans were acquired with a camera line rate of 1 kHz. The power dissipated on the electromagnet was 100 W, corresponding to a power supply control voltage of 7.5 V. The period of a cycle was about 25 ms, with a duty cycle of 32%. Thus, the magnetic field was modulated at 40 Hz. The results of this experiment indicate that the time scale of the sample response to magnetic field changes (either displacing when the field is turned on, or relaxing when the field is turned off), is comparable to if not larger than the duration of a cycle. It is difficult to assess if the agents and the sample have enough time to complete motion and reach equilibrium with the present magnetic field modulation period. Therefore, in order to better evaluate these time scales, measurements of magnetomotion with the magnetic field modulated at lower frequencies were done subsequently and are discussed below. Nonetheless, magnetomotion is evident in the data shown in Fig. 4.

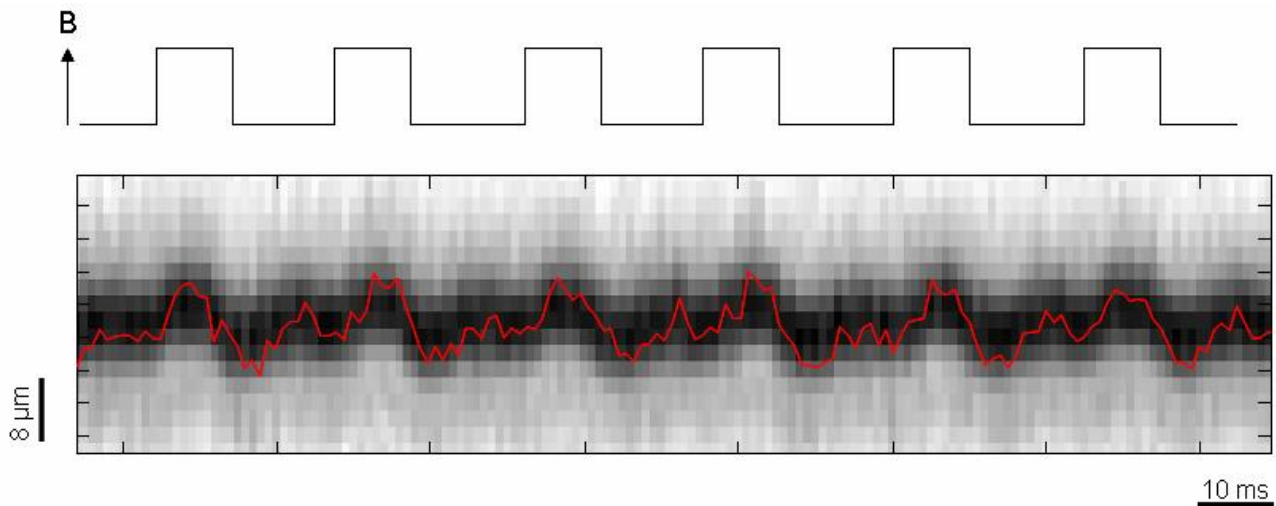


Figure 4: Amplitude (grey-scale pixelated) and group delay (fine solid line) in M-mode from the top surface of a tissue-like sample containing magnetic nanoparticles (bottom) while the magnetic field is turned on and off periodically (top).

This is the first evidence of the detection of magnetomotion in the SD-OCT system. The fluctuations in the amplitude and in the group delay of the unwrapped phase correspond to the state of the sample when the magnetic field is being modulated, and thus the magnetic nanoparticles in the sample have moved along the axial direction, engaging the sample in an axial displacement. The stability of the phase allows for the unwrapping of the phase and

thus the calculation of the group delay.²⁹ The phase sensitivity in the system was calculated as the standard deviation of the phase from a perfect reflector¹⁰ (mirror) and was found to be 0.18 rad. In terms of physical displacement and given the bandwidth and the center wavelength of our source, and a refractive index of approximately 1.4 for the phantom, this translates to approximately an 8 nm displacement sensitivity. These values of sensitivity are larger than those reported for spectral-domain phase microscopy most likely because our SD-OCT system is a dual-path interferometer and thus the phase stability is vulnerable to jitter in the relative path lengths and other noise sources that common-path systems can significantly reduce.¹⁰⁻¹² Compared to time-domain phase stability, however, this is an important improvement (for example, a time-domain OCT system with Fourier domain optical delay using a resonant scanning mirror exhibits a phase stability of ~1 rad at 100 Hz).

The magnetic nanoparticles are engaged in transient motion when the field is turned either on or off, tending towards an equilibrium position. When the field is on the magnetic nanoparticles and the surrounding tissue are in a tensile state, and when the field is turned off, they are relaxing. In order to better assess the time scales of the motion of particles during the two transitions we need to allow them to reach a state of equilibrium.⁸ For this purpose, the magnetic field was modulated at a lower frequency than in the previous experiment, namely 6.67 Hz, while the camera rate was kept at 1 kHz. The amplitude and unwrapped phase M-mode data are shown in Fig. 5. From the amplitude image alone (top of Fig. 5) it might appear that at this frequency of the magnetic field the particles have enough time to reach an equilibrium position after both transitions. However, the averaged absolute value of the amplitude difference with respect to a background (zero-magnetic field) value for each row and the corresponding averaged unwrapped phase shift, defined as

$$a_{frac}(t) = \frac{mean_z |a(z,t) - mean_{t_beforeBon}(a(z,t))|}{mean_z(a(z,t))} \quad (1)$$

and

$$\phi_{frac}(t) = \frac{mean_z |\phi(z,t) - mean_{t_beforeBon}(\phi(z,t))|}{mean_z(\phi(z,t))}, \quad (2)$$

and plotted in the middle graph in Fig. 5, show that the scatterers appear to be exhibiting damped oscillations immediately after the changes in the magnetic field occur. The scatterers overshoot the equilibrium position as the result of the momentum they acquire, but then the amplitude of the oscillations decreases significantly because of energy dissipation in the system. This result constitutes the basis for dynamic studies of these oscillations. The phase modulation and the amplitude modulation are in good agreement. The repeatability of the oscillation as the magnetic field is being modulated is reassuring, as confirmed by Fourier analysis of the data. This data indicates that the strongest achievable MMOCT signal can be captured within a few milliseconds of the onset of the magnetic field (in this case, the mean time between onset of magnetic field and maximum displacement is 7 ms), but this will be dependent on the regional micromechanical properties of the sample or tissue. Further investigation of these oscillations with lower magnetic field frequencies is needed in order to fully characterize them and to ensure that they are a signature of the probed material. The control data for the non-magnetic phantom in the presence of the magnetic field modulation is shown in the lower graph in Fig.5. The power spectra of both amplitude and phase data for this sample do not have peak components at 6.67 Hz, as expected, since the magnetic field should not trigger a response in a non-magnetic sample. The phase drift over time is apparent in both the magnetic sample and the control data, while the amplitude has a steady profile throughout the entire scan. This suggests that phase measurements should utilize correction methods for measurements over longer times.²⁹

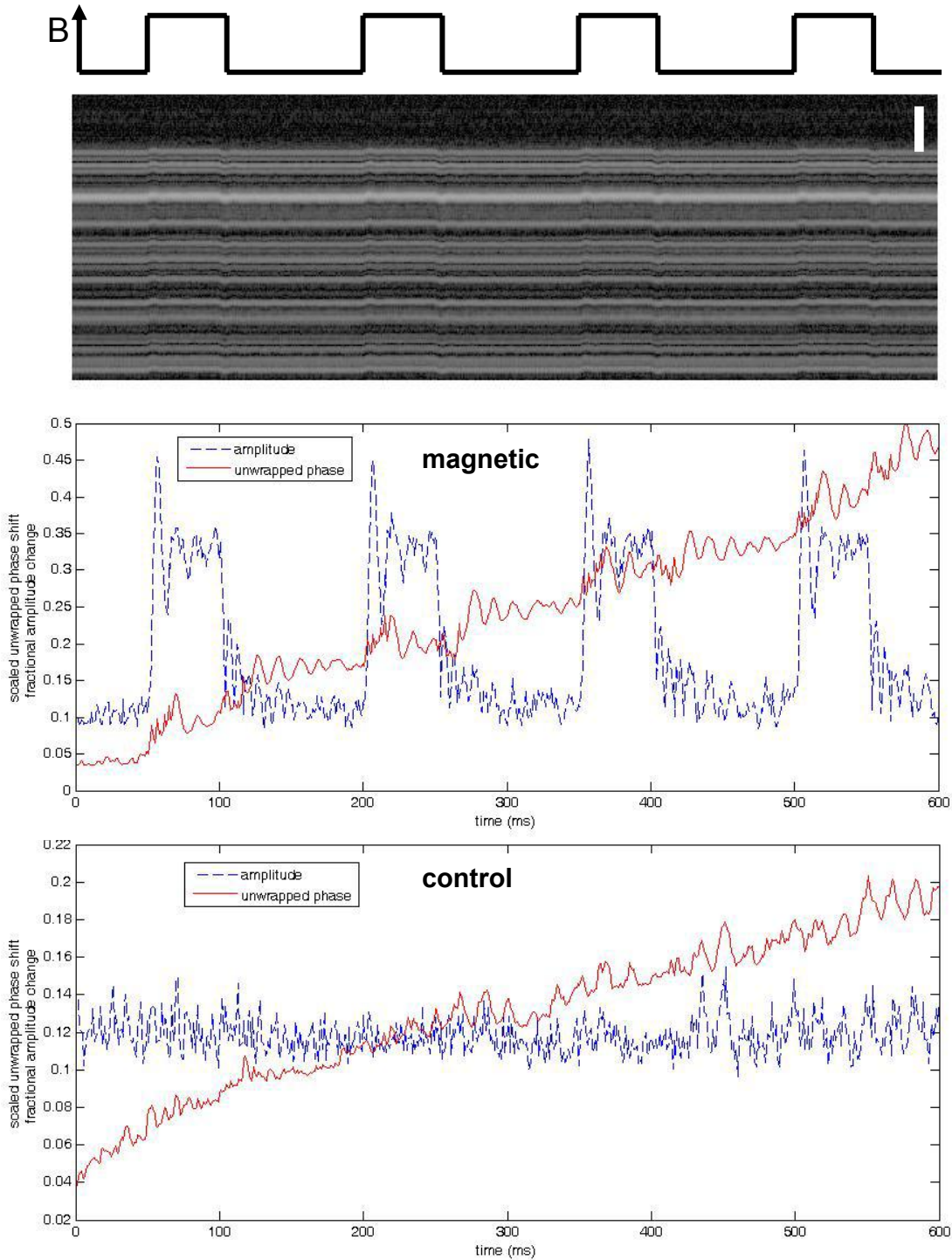


Figure 5: M-mode magnetomotive SD-OCT data for a magnetic and a control sample with the magnetic field modulated at 6.67 Hz, camera line rate 1 kHz, and electromagnet control voltage of 7.5 V. Top: depth varying amplitude image (vertical scale bar = 0.3 mm) for the magnetic sample. Middle: fractional mean of absolute value amplitude variation and scaled mean unwrapped phase variation over all rows for the magnetic sample (according to Eqs. 1 and 2). Bottom: fractional mean of absolute value amplitude variation and scaled mean unwrapped phase variation over all rows for the control sample.

In another experiment, the magnetic field strength was varied by changing the electromagnet power, and 8100 axial scans were acquired with a camera line rate of 29 kHz. This high frequency allows for higher sampling of the oscillations at the transitions between different states of the magnetic field. The magnetic field was modulated at 11.6 Hz in order to accommodate a set of three off-on transitions over the whole duration of a scan, which was 279.3 ms. The magnetic field strength is proportional to the power supply control voltage. The results of this experiment for a magnet control voltage of 7.5 V were in good agreement with those of Fig. 5, with the advantage of better resolution, as evidenced in Fig. 6.

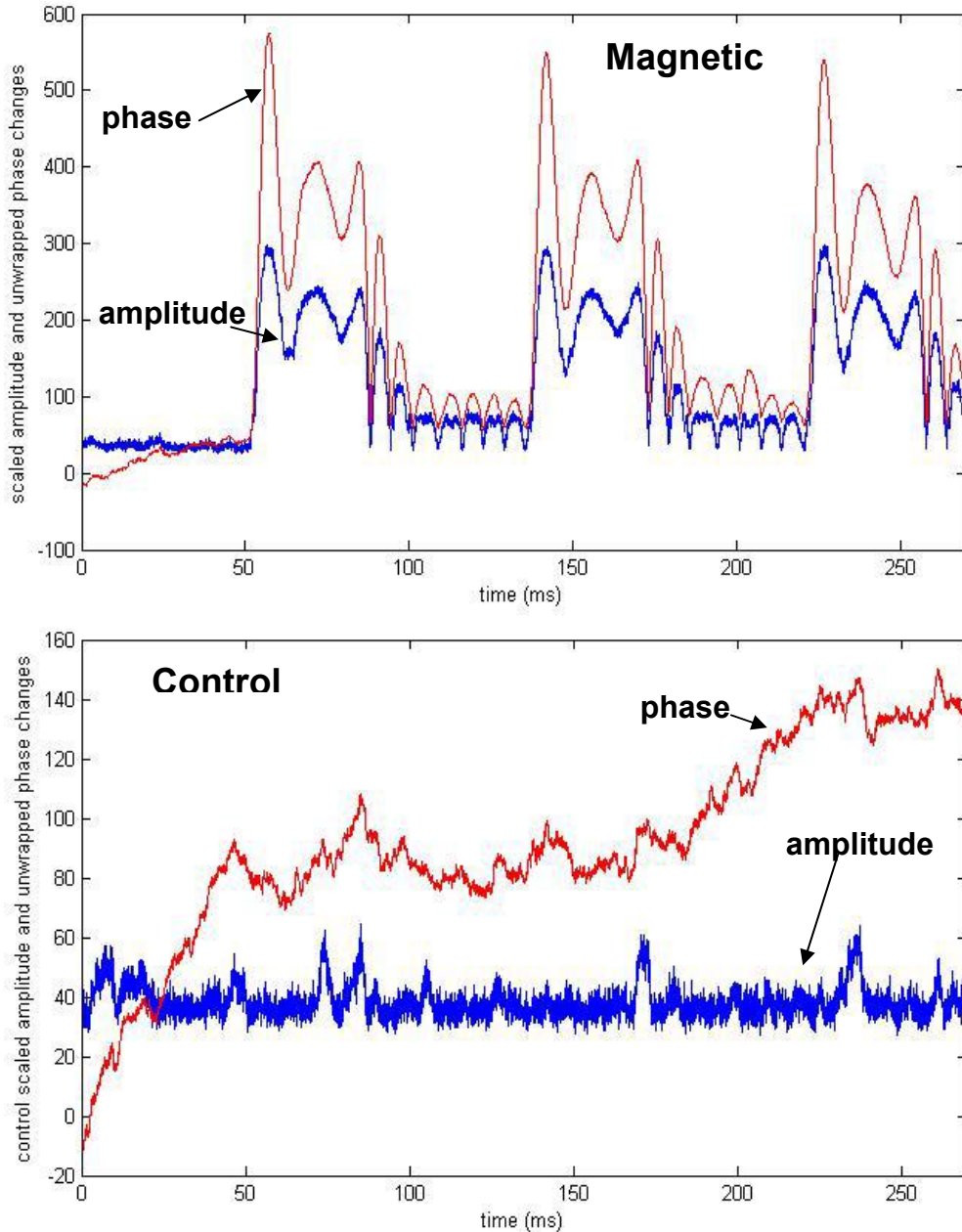


Figure 6: M-mode magnetomotive SD-OCT amplitude and phase changes (according to Eqs. 1 and 2) with the magnetic field modulated at 11.6 Hz, camera line rate 29 kHz, and electromagnet control voltage of 7.5 V. Top: Magnetic sample. Bottom: Control sample.

The changes in amplitude and phase in response to different strengths of magnetic field are plotted in Fig. 6. The maximum MMOCT amplitude and phase changes were calculated as the differences between the corresponding values at the displacement peak immediately after the magnetic field is turned on and the mean values of phase and amplitude right before that. As expected, both amplitude and phase changes increase with the field, corresponding to an increase in the displacements in the sample.

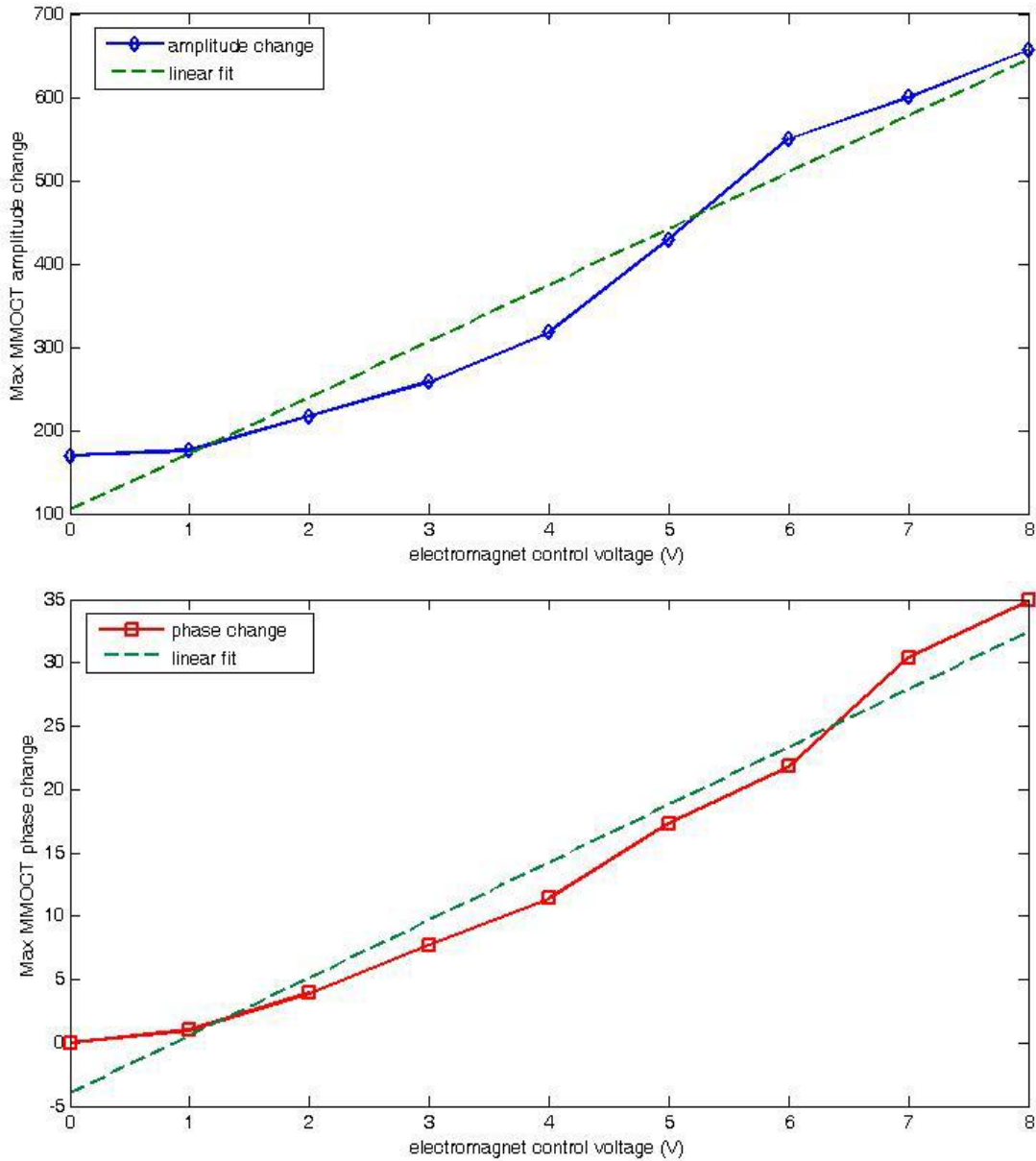


Figure 7: Maximum MMOCT amplitude (top) and phase response (bottom) vs. electromagnet control voltage

Phase and amplitude changes for a low magnetic field corresponding to a control voltage of 1 V reveal the smallest displacement detected in this set of data. The amplitude and phase variations right before and after the magnetic field is turned on are plotted in Fig. 8. The amplitude data at this low value of the field becomes quite noisy, while the profile of the unwrapped phase is still smooth, suggesting more sensitive detection from phase analysis than from amplitude analysis. This may be close to the delineating zone between regimes in which phase versus amplitude

measurements are preferred. We calculated the sensitivities for this data as the changes in amplitude and phase immediately after the field was turned on, relative to the idle state of the sample right before the field was turned on (averaging for before and after onset of field was done over ~ 1 ms), divided by the standard deviation of their value over the same period of non-magnetic activity. The phase signal-to-noise ratio was found to be 23.20 and the amplitude signal-to-noise ratio was 7.72, showing that in this regime phase analysis is preferable.

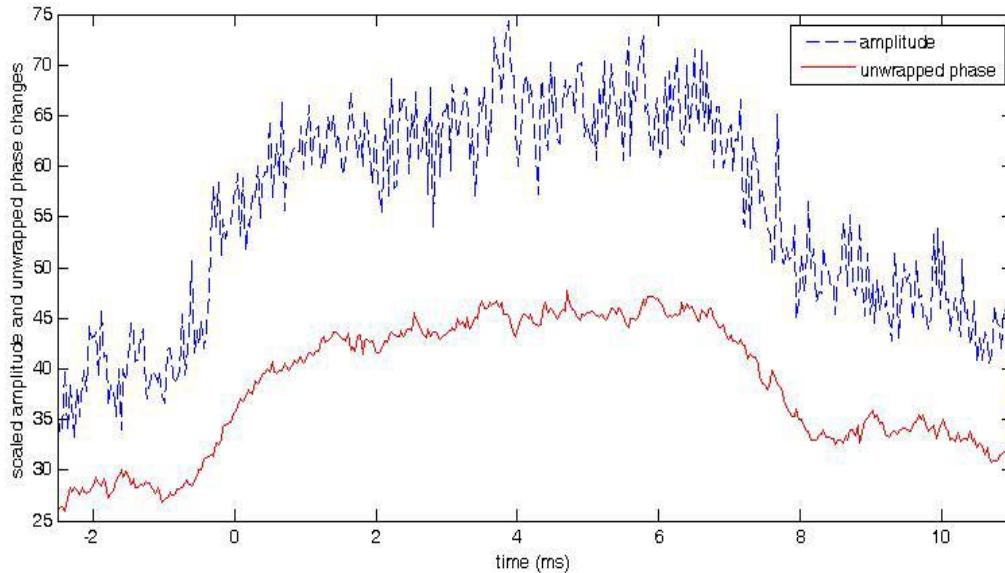


Figure 8: M-mode magnetomotive SD-OCT amplitude and phase changes (according to Eqs. 1 and 2) with the magnetic field modulated at 11.6 Hz, camera line rate 29 kHz, and electromagnet control voltage of 1 V.

CONCLUSIONS

We have shown that magnetomotive OCT is achievable with spectral-domain OCT detection techniques and could benefit from the fast acquisition rates of the system for studying the dynamics of magneto-motion. One major advantage of this system compared to TD-OCT is improved phase stability that allows analysis of motion that might not be detectable with amplitude and opens a potential venue for characterization of magnetic nanoparticles dynamic behavior and tissue elasticity, concurrently. These results lay the foundation for further investigation of phase and amplitude modulations in response to a varying magnetic field in a sample in which magnetic nanoparticles are embedded. The versatility of these particles is promising as contrast agents for imaging and possibly therapeutic use once targeting and functionalization are achieved.

REFERENCES

1. D. Huang, E.A. Swanson, C.P. Lin, J.S. Schuman, W.G. Stinson, W. Chang, M.R. Hee, T. Flotte, K. Gregory, C.A. Puliafito, and J.G. Fujimoto, "Optical Coherence Tomography," *Science* **254**, 1178 (1991).
2. A.F. Fercher, W. Drexler, C.K. Hitzenberger, and T. Lasser, "Optical Coherence Tomography -- principles and applications," *Rep. Prog. Phys* **66** 239(2003).
3. S.A. Boppart, A.L. Oldenburg, C. Xu, and D.L. Marks, "Optical probes and techniques for molecular contrast enhancement in coherence imaging," *J. Biomed. Opt.*, 10:041208 (2005).
4. A.L. Oldenburg, J.R. Gunther, and S.A. Boppart, "Imaging magnetically labeled cells with magnetomotive optical coherence tomography," *Opt. Lett.* **30**, 747-749 (2005).
5. A.L. Oldenburg, J.R. Gunther, F. Jean-Jacques Toublan, D.L. Marks, K.S. Suslick, and S.A. Boppart, "Selective OCT imaging of cells using magnetically-modulated optical contrast agents," in *Proceedings of the*

- Conference on Lasers and Electro-Optics*, pp. 405-406 (2003).
6. R. Kopelman, Y.-E. L. Koo, M. Philbert, B.A. Moffat, G.R. Reddy, P. McConville, D.E. Hall, T.L. Chenevert, M.S. Bhojani, S.M. Buck, A. Rehemtulla, and B.D. Ross, "Multifunctional nanoparticle platforms for in vivo MRI enhancement and photodynamic therapy of a rat brain cancer, ", *J. Magn. Magn. Mat.* **252**, 404 (2005).
 7. E. Romanus, M. Huckel, C. Gross, S. Prass, W. Weitschies, R. Brauer, and P. Weber, "Magnetic nanoparticle relaxation measurement as a novel tool for in vivo diagnostics, " *J. Magn. Magn. Mat.* **293**, 387 (2002).
 8. A.L. Oldenburg, F.J.J. Toublan, K.S. Suslick, A. Wei, and S.A. Boppart, "Magnetomotive contrast for in vivo optical coherence tomography," *Opt. Express* **13**, 6597-6614 (2005).
 9. J. Oh, M.D. Feldman, J. Kim, C. Condit, S. Emelianov, and T.E. Milner, "Detection of magnetic nanoparticles in tissue using magneto-motive ultrasound, " *Nanotechnology* **17**, 4183-4190 (2006).
 10. C. Joo, T.A. Akkin, B. Cense, B.H. Park, and J.F. de Boer, "Spectral-domain optical coherence phase microscopy for quantitative phase-contrast imaging," *Opt. Lett.* **30**, 16 (2005).
 11. M.A. Choma, A. K. Ellerbee, C. Yang, T.L. Creazzo, and J.A. Izatt, "Spectral-domain phase microscopy," *Opt. Lett.* **30**, 1162-1164 (2005).
 12. M.A. Choma, A. K. Ellerbee, S. Yazdanfar, and J.A. Izatt, "Doppler flow imaging of cytoplasmic streaming using spectral domain phase microscopy," *J. Biomed. Opt.* **11**(2), 024014 (2006).
 13. M. Sticker, M. Pircher, E. Götzinger, H. Sattmann, A. F. Fercher, and C.K. Hitzenberger, "En face imaging of single cell layers by differential phase-contrast optical coherence tomography, " *Opt. Lett.* **27**, 13 (2002).
 14. M. V. Sarunic, S. Weinberg, and J.A. Izaat, "Full-field swept-source phase microscopy, " *Opt. Lett.* **31**, 10 (2006).
 15. M. H. De la Torre-Ibarra, P.B. Ruiz, and J.M. Huntley, "Double-shot depth-resolved displacement field measurement using phase-contrast spectral coherence tomography, " *Opt. Express* **14**, 9643-9656 (2006).
 16. B.J. Vakoc, S.H. Yun, J.F. de Boer, G.J. Tearney, and B.E. Bouma, "Phase-resolved optical frequency domain imaging, " *Opt. Express* **13**, 5483-5493 (2005).
 17. C.J. Pedersen, S. Yazdanfar, V. Westphal, and A.M. Rollins, "Phase-referenced Doppler optical coherence tomography in scattering media, " *Opt. Lett.* **30**, 16 (2005).
 18. H. Ren, K.M. Brecke, Z. Ding, Y. Zhao, J.S. Nelson, and Z. Chen, "Imaging and quantifying transverse flow velocity with the Doppler bandwidth in a phase-resolved functional optical coherence tomography, " *Opt. Lett.* **27**, 6 (2002).
 19. Y. Zhao, Z. Chen, C. Saxer, Q. Shen, S. Xiang, J.F. de Boer, and J.S. Nelson, "Doppler standard deviation imaging for clinical monitoring of in vivo human skin blood flow, " *Opt. Lett.* **25**, 18 (2000).
 20. H. Ren, Z. Ding, Y. Zhao, J. Miao, J.S. Nelson, and Z. Chen, "Phase-resolved functional optical coherence tomography: simultaneous imaging of in situ tissue structure, blood flow velocity, standard deviation, birefringence, and Stokes vectors in human skin, " *Opt. Lett.* **27**, 27 (2002).
 21. Z. Ding, Y. Zhao, H. Ren, J.S. Nelson, and Z. Chen, "Real-time phase-resolved optical coherence tomography and optical Doppler tomography, " *Opt. Express* **10**, 236-244(2002).
 22. B.R. White, M.C. Pierce, N. Nassif, B. Cense, B. Hyle Park, G.J. Tearney, and B.E. Bouma, "In vivo dynamic human retinal blood flow imaging using ultra-high-speed spectral domain optical Doppler tomography, ", *Opt. Express* **11**, 3490-3496 (2003).
 23. H. Ren, T. Sun, D.J. MacDonald, M.J. Cobb, and X. Li, "Real-time in vivo blood-flow imaging by moving-scatterer-sensitive spectral-domain optical Doppler tomography," *Opt. Lett.* **31**, 7 (2006).
 24. C. Fang-Yen, M.C. Chu, H.S. Seung, R.R. Dasari, and M.S. Feld, "Noncontact measurement of nerve displacement during action potential with a dual-beam low-coherence interferometer, " *Opt. Lett.* **29**, 17(2004).
 25. M.A. Choma, M.V. Sarunic, C. Yang, and J.A. Izatt, "Sensitivity advantage of swept source and Fourier domain optical coherence tomography," *Opt. Express* **11**, 2183-2189 (2003).
 26. R. Leitgeb, C.K. Hitzenberger, and A.F. Fercher, "Performance of fourier domain vs. time domain optical coherence tomography," *Opt. Express* **11**, 889-894 (2003).
 27. R.A. Leitgeb, W. Drexler, A. Unterhuber, B. Hermann, T. Bajraszewski, T. Le, A. Stingl, and A.F. Fercher, "Ultrahigh resolution Fourier domain optical coherence tomography, " *Opt. Express* **12**, 2156-2165 (2004).
 28. J.F. De Boer, B. Cense, B.H. Park, M.C. Pierce, G.J. Tearney, and B.E. Bouma, "Improved signal-to-noise ratio in spectral-domain compared with time-domain optical coherence tomography, " *Opt. Lett.* **28**, 2067-2069 (2003).
 29. T.S. Ralston, D.L. Marks, P.S. Carney, and S.A. Boppart, "Phase Stability Technique for Inverse Scattering in Optical Coherence Tomography," *International Symposium on Biomedical Imaging*, 578 – 581 (2006).